TECHNICAL RESEARCH REPORT

SYSTEMS RESEARCH CENTER

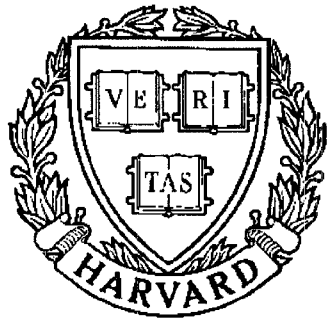

Supported by the National Science Foundation Engineering Research Center Program (NSFD CD 8803012), Industry and the University

Dynamic Bifurcations in a Power System Model Exhibiting Voltage Collapse

by E.H. Abed, J.C. Alexander, H. Wang, A.M.A. Hamdan, and H-C. Lee

TR 92-26

Manuscript: Feb. 25, 1992

Dynamic Bifurcations in a Power System Model Exhibiting Voltage Collapse

E.H. Abed* J.C. Alexander† H. Wang* A.M.A. Hamdan‡

H.-C. Lee§

Keywords: Power systems, voltage collapse, bifurcation, stability, oscillations, chaos.

Abstract

Dynamic bifurcations, including Hopf and period-doubling bifurcations, are found to occur in a power system dynamic model recently employed in voltage collapse studies. The occurrence of dynamic bifurcations is ascertained in a region of state and parameter space linked with the onset of voltage collapse. The work focuses on a power system model studied by Dobson and Chiang (1989). The presence of the dynamic bifurcations, and the resulting implications for dynamic behavior, necessitate a re-examination of the role of saddle node bifurcations in the voltage collapse phenomenon. The bifurcation analysis is performed using the reactive power demand at a load bus as the bifurcation parameter. Due to numerical ill-conditioning, a reduced-order model is employed in some of the computations. It is determined that the power system model under consideration exhibits two Hopf bifurcations in the vicinity of the saddle node bifurcation. Between the Hopf bifurcations, i.e., in the "Hopf window," period-doubling bifurcations are found to occur. Simulations are given to illustrate the various types of dynamic behaviors associated with voltage collapse for the model. In particular, it is seen that an oscillatory transient may play a role in the collapse.

*Department of Electrical Engineering and the Systems Research Center, University of Maryland, College Park, MD 20742 USA

†Department of Mathematics, University of Maryland, College Park, MD 20742 USA

‡Department of Electrical Engineering, Jordan University of Science and Technology, Irbid, Jordan

§Chung Shan Inst. Sci. and Technol., Lung-Tan, Taiwan, R.O.C.

1 Introduction

Voltage collapse in electric power systems has recently received significant attention in the literature (see, e.g., [1] for a synopsis). This has been attributed to increases in demand which result in operation of an electric power system near its stability limits. A number of physical mechanisms have been identified as possibly leading to voltage collapse. From a mathematical perspective, voltage collapse has been viewed as arising from a *bifurcation* of the power system governing equations as a parameter is varied through some critical value. In several papers (e.g., [2], [12], [6], [17], [7]), voltage collapse is viewed as an instability which coincides with the disappearance of the steady state operating point as a system parameter, such as a reactive power demand, is quasistatically varied. In the language of bifurcation theory, these papers link voltage collapse to a *fold* or *saddle node bifurcation* of the nominal equilibrium point.

Dobson and Chiang [2] presented a mechanism for voltage collapse which postulates that this phenomenon occurs at a saddle node bifurcation of equilibrium points. They employed the Center Manifold Theorem to understand the ensuing dynamics. In the same paper, they introduced a simple example power system containing a generator, an infinite bus and a nonlinear load (see Figure 1). The saddle node bifurcation mechanism for voltage collapse postulated in [2] was investigated for this example in [2] and in [12].

An essential distinction exists between the mathematical formulation of voltage collapse problems and transient stability problems. In studying transient stability, one often is interested in whether or not a given power system can maintain synchronism (stability) after being subjected to a physical disturbance of moderate or large proportions. The faulted power system in such a case has been perturbed in a severe way from steady-state, and one studies the possibility of the post-fault system returning to steady-state (regaining synchronism). In the voltage collapse scenario, however, the disturbance may be viewed as a slow change in a system parameter, such as a power demand. Thus, the disturbance does not necessarily perturb the system away from steady-state. The steady-state varies continuously with the changing system parameter, until it disappears at a saddle node bifurcation point. It is therefore not surprising that saddle node bifurcation is being studied as a possible route

to voltage collapse.

However, another possibility is that the steady-state operating point loses stability *before the saddle node bifurcation.* If this occurs in a given system, an important implication is that the margin of stability, i.e., the distance in parameter space to the stability boundary, will be less than one might expect if saddle node bifurcation were taken as the determinant of voltage collapse. Stability of the nominal equilibrium point may be lost prior to the saddle node bifurcation through a Hopf bifurcation. Hopf bifurcation has indeed been found previously in power system models; see for instance [18], [19], [20]. Hopf bifurcation requires a complex conjugate pair of eigenvalues to cross the imaginary axis for some parameter value. Hopf bifurcation, like saddle node bifurcation, is a generic occurrence in one-parameter families of differential systems. It results in the appearance of a family of small-amplitude periodic solutions. For details, see for instance [9], [10], [11].

In this paper, we consider the latter possibility noted in the preceding paragraph by exploring it for the example of [2]. We show that even this simple example admits *dynamic bifurcations* in addition to the saddle node bifurcation studied in [2] and [12]. These dynamic bifurcations include Hopf bifurcation [9], [10], cyclic fold bifurcation [11] and period doubling bifurcation [11], [8] . These bifurcations all involve periodic solutions of the system under consideration. The results for this example are obtained using the bifurcation analysis software package AUTO [15] and the nonlinear system simulation tool kaos [16].

This paper continues the investigation of [3], where the presence of Hopf bifurcations in the example model of [2] was first reported. The main results of the present paper appear also in the authors' recent paper [4]. After completion of our paper [4], we learned of the recent work [5], which addresses the same model as that considered here, while emphasizing the presence of chaotic solutions. In contrast, our emphasis is on the implications of the bifurcations observed on voltage collapse. However, as in [4], we note that the occurrence of period doubling bifurcations is a common signal for the presence of chaotic motion [8], and the model under study is no exception. Note that the existence of chaotic invariant sets in power system models has been ascertained previously in the literature; see for instance [13] and [14]. See also reference [5].

In the course of this work, numerical ill-conditioning was observed for the dynamic equa-

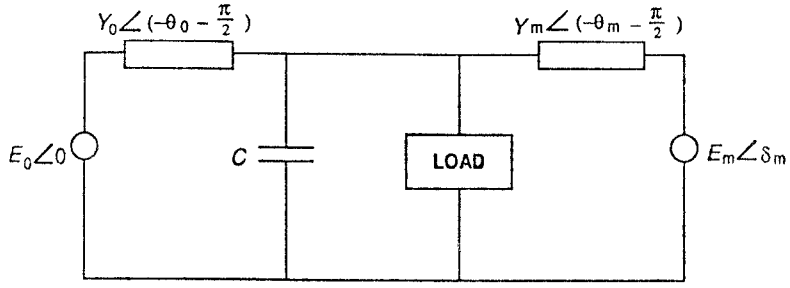

Figure 1: Power system model.

tions of the example power system studied in [2]. This is an artifact of the model under study, rather than an expected feature of more realistic power system models. Nevertheless, it was felt that further analysis of the bifurcation behavior of this model was called for. To alleviate the numerical difficulties, in performing the bifurcation analysis the fastest variable in the model is eliminated through a singular perturbation argument. However, simulations of both the original and reduced system are presented. The simulations show that little is lost from a qualitative point of view in the model reduction.

Since this study concentrates on the particular example power system given in [2], detailed accuracy was not considered to be a main issue. Rather, the goal of this work is to show the richness of the qualitative behaviors which may occur near voltage collapse, and to illustrate their effect on system trajectories.

The organization of this paper is as follows. In the next section, we recall the model power system considered in [2], and give a reduced order version of that model. In Section 3, bifurcations occurring for the reduced model and the original model are studied. In Section 4, simulation results are presented which illustrate various effects of the bifurcations of Section 3. Conclusions are collected in Section 5.

2 The Model

The power system under consideration in this paper, previously considered by Dobson and Chiang [2], is depicted in Figure 1. The three nodes of the equivalent circuit in Fig. 1 are

an infinite busbar, a generator node represented by a constant voltage behind a reactance, and a load busbar. The system dynamics is governed by the following four differential equations [2] ($P(\delta, V)$, $Q(\delta, V)$ are specified below):

$$\dot{\delta}_m = \omega \tag{1}$$

$$M\dot{\omega} = -d_m\omega + P_m + E_m V Y_m \sin(\delta - \delta_m - \theta_m) + {E_m}^2 Y_m \sin\theta_m \tag{2}$$

$$K_{qw}\dot{\delta} = -K_{qv2}V^2 - K_{qv}V + Q(\delta, V) - Q_0 - Q_1 \tag{3}$$

$$TK_{qw}K_{pv}\dot{V} = K_{pw}K_{qv2}V^2 + (K_{pw}K_{qv} - K_{qw}K_{pv})V + K_{qw}(P(\delta, V) - P_0 - P_1) - K_{pw}(Q(\delta, V) - Q_0 - Q_1) \tag{4}$$

All symbols used are the same as in [2]. The load includes a constant PQ load in parallel with an induction motor. The real and reactive powers supplied to the load by the network are

$$P(\delta, V) = -E'_0 V Y'_0 \sin(\delta + \theta'_0) - E_m V Y_m \sin(\delta - \delta_m + \theta_m) + (Y'_0 \sin\theta'_0 + Y_m \sin\theta_m)V^2 \tag{5}$$

$$Q(\delta, V) = E'_0 V Y'_0 \cos(\delta + \theta'_0) + E_m V Y_m \cos(\delta - \delta_m + \theta_m) + (Y'_0 \cos\theta'_0 + Y_m \cos\theta_m)V^2 \tag{6}$$

2.1 The Reduced Model

As noted above, the model (1)-(6) presents significant numerical ill-conditioning. To circumvent this, we reduce the dimensionality of this model by eliminating from it the variable δ. This is justified for the data used in [2], since K_{qw} is small in comparison with other system data. The resulting reduced order model is

$$\dot{\delta}_m = \omega \tag{7}$$

$$M\dot{\omega} = -d_m\omega + P_m + E_m V Y_m \sin(\delta - \delta_m - \theta_m) + {E_m}^2 Y_m \sin\theta_m \tag{8}$$

$$TK_{pv}\dot{V} = -K_{pv}V - P_0 - P_1 + P(\delta_e, V) \tag{9}$$

where

$$P(\delta_e, V) = -E_0' V Y_0' \sin(\delta_e + \theta_0')$$
$$-E_m V Y_m \sin(\delta_e - \delta_m + \theta_m) + (Y_0' \sin\theta_0' + Y_m \sin\theta_m)V^2 \quad (10)$$

$$\delta_e = -\cos^{-1}\left(\frac{S}{\sqrt{K_{i1}^2 + K_{i2}^2}}\right) + \cos^{-1}\left(\frac{K_{i1}}{\sqrt{K_{i1}^2 + K_{i2}^2}}\right) \quad (11)$$

$$S = Q_0 + Q_1 + K_{qv}V + K_{qv2}V^2$$
$$+(Y_0' \cos\theta_0' + Y_m \cos\theta_m)V^2 \quad (12)$$

$$K_{i1} = E_0' V Y_0' \cos\theta_0' + E_m V Y_m \cos(\theta_m - \delta_m) \quad (13)$$

$$K_{i2} = -E_0' V Y_0' \sin\theta_0' - E_m V Y_m \sin(\theta_m - \delta_m) \quad (14)$$

3 Bifurcations

In this section, the results of a bifurcation analysis of the third order reduced model (7)-(14) are given, and implications for both the reduced system and the full model (1)-(6) are discussed. The values we employ for the parameters appearing in the equations above are the same as those given in [2].

A bifurcation diagram for the third order reduced model (7)-(14) appears in Figure 2. This diagram relates the voltage magnitude V to the reactive power demand Q_1. Essential features of the bifurcation diagram are now summarized. To simplify the discussion, note first that in Fig. 2 there are six bifurcations depicted. These are labeled HB①, CFB②, PDB③, PDB④, HB⑤ and SNB⑥. For simplicity, we may also refer to these bifurcations through their numbers ①-⑥, respectively. The acronyms have the following meanings:

- HB: Hopf bifurcation
- CFB: Cyclic fold bifurcation
- PDB: Period doubling bifurcation
- SNB: Saddle node bifurcation

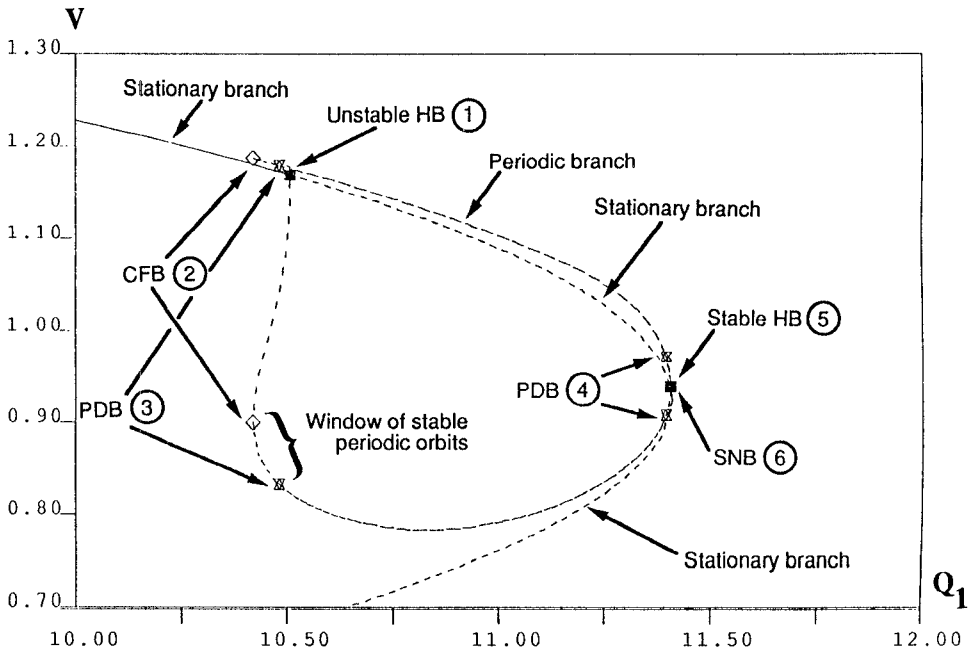

Figure 2: Bifurcation diagram for reduced model.

For ease of reference, we denote the values of the parameter Q_1 at which the bifurcations ①-⑥ occur by $Q_1^{①}$-$Q_1^{⑥}$, respectively. For $Q_1 < Q_1^{①}$, a stable equilibrium point exists with voltage magnitude in the neighborhood of 1.2. (Upper left in Fig. 2.) As Q_1 is increased, an unstable ("subcritical") Hopf bifurcation is encountered at the point labeled HB① in Fig. 2. As Q_1 is increased further, the stationary point regains stability at $Q_1 = Q_1^{⑤}$ through a stable ("supercritical") Hopf bifurcation. This stable equilibrium merges with another, unstable stationary branch and disappears in the saddle node bifurcation labeled SNB⑥ in Fig. 2. The numerical computations show that the family of periodic solutions emerging from the Hopf bifurcation at ① and the family of periodic solutions emerging from the Hopf bifurcation at⑤ are one and the same.

Besides the bifurcations of the nominal equilibrium described in the foregoing, the periodic solutions emerging from the Hopf bifurcations at ① and ⑤ themselves undergo bifurcations. Determining the location and nature of all of the associated bifurcations is not an easy computational task, since it involves using numerical continuation to follow the bifurcated periodic solutions, as well as other solutions bifurcated from them, and so on. However, we discuss a few of these bifurcations to give an idea of the possibilities.

Since HB① is a subcritical Hopf bifurcation, it results in a family of unstable periodic solutions occurring for Q_1 slightly less than $Q_1^{①}$. In Fig. 2, the envelope of this family of periodic solutions in the variable V is indicated by the pair of dashed curves appearing from ① and extending to the left. At $Q_1 = Q_1^{②}$, the unstable periodic solution undergoes a *cyclic fold bifurcation.* Thus, in Fig. 2, the continuation of the dashed curve of periodic solutions for Q_1 near $Q_1^{②}$ exists for Q_1 slightly greater than $Q_1^{②}$. A cyclic fold bifurcation is simply a saddle node bifurcation of periodic solutions. Thus, the unstable periodic solution gains stability at $Q_1 = Q_1^{②}$.

Simulation evidence indicates that the bifurcation diagram of Fig. 2 is qualitatively the same for the original fourth order model. In other words, the two Hopf bifurcations, the period doubling bifurcations, and the cyclic fold bifurcation also occur in the fourth order model. The main difference in the respective bifurcation diagrams is the parameter interval (i.e., the range of values of Q_1) over which the bifurcation sequence takes place. This interval is smaller for the fourth order model than it is for the third order model, and closer to the saddle node bifurcation. To illustrate this, some bifurcation parameter values are noted next. These are approximate – it was not felt that more detailed calculations were justified. The parameter value $Q_1^{①}$ at the first Hopf bifurcation (HB① in Fig. 2) is approximately 10.5 in the third order model, while simulations show it to be in the range 10.925-10.95 for the fourth order model. The parameter value $Q_1^{⑤}$ at which the second Hopf bifurcation occurs at approximately 11.408 in the third order model, and is in the range 11.406-11.407 for the fourth order model.

The original and reduced models show good agreement in a range very close to the saddle node bifurcation. Indeed, the second Hopf bifurcation is supercritical for both models. For $Q_1^{⑤} < Q_1 < Q_1^{⑥}$, i.e., just before the saddle node bifurcation SNB⑥, the equilibrium is stable. This holds both for the reduced and the full model. Thus, in a sufficiently small neighborhood of the parameter value $Q_1^{⑥}$, the system remains at the steady-state if its initial condition is at the nominal equilibrium. This is in agreement with the results of [2] and [12]. Of course, it is also true that the system would in all likelihood *not* be operating at this equilibrium, due to the effects of the bifurcations discussed above.

The appearance of a window of stable large amplitude periodic orbits (see Fig. 2) in

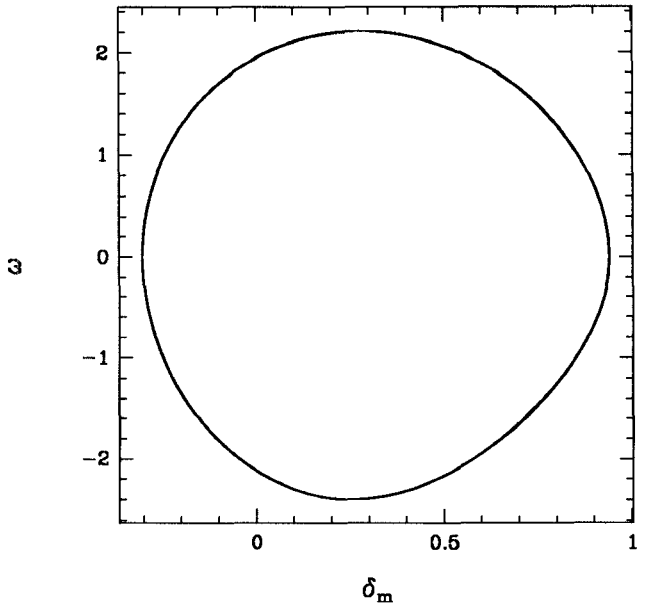

Figure 3: A stable large amplitude periodic orbit for $Q_1 = 10.45$.

the parameter range $Q_1^{②} < Q_1 < Q_1^{③}$ as a result of the cyclic fold bifurcation CFB② can be verified by careful simulation. Indeed, Fig. 3 shows (for the third order model) a stable periodic orbit which belongs to this family, occurring for $Q_1 = 10.45$. (The initial condition used to generate this orbit is $(\delta_m = -0.3, \omega = -0.001, V = 0.89)$.)

This stable large-amplitude orbit loses stability at the *period doubling bifurcation* PDB③. At this bifurcation, a new periodic orbit appears which initially coincides with the original orbit, except that it is of exactly twice the period. The original orbit necessarily loses stability at such a bifurcation. The branch of period-doubled orbits is not shown in Fig. 2, nor any further bifurcations from that branch. However, note that another period doubling bifurcation is found to occur from the periodic orbits emanating from HB⑤; this bifurcation is labeled PDB④ in Fig. 2.

Simulations of the system in the parameter range corresponding to the "Hopf window" indicate the presence of further bifurcations of periodic orbits, and of aperiodic (chaotic) orbits. This is expected [8]. There are further period doublings (not shown) just beyond the period doublings PDB indicated in the figure. This indicates there is a period doubling cascade, with the resulting chaotic orbit. Indeed one surmises there are an infinite number of

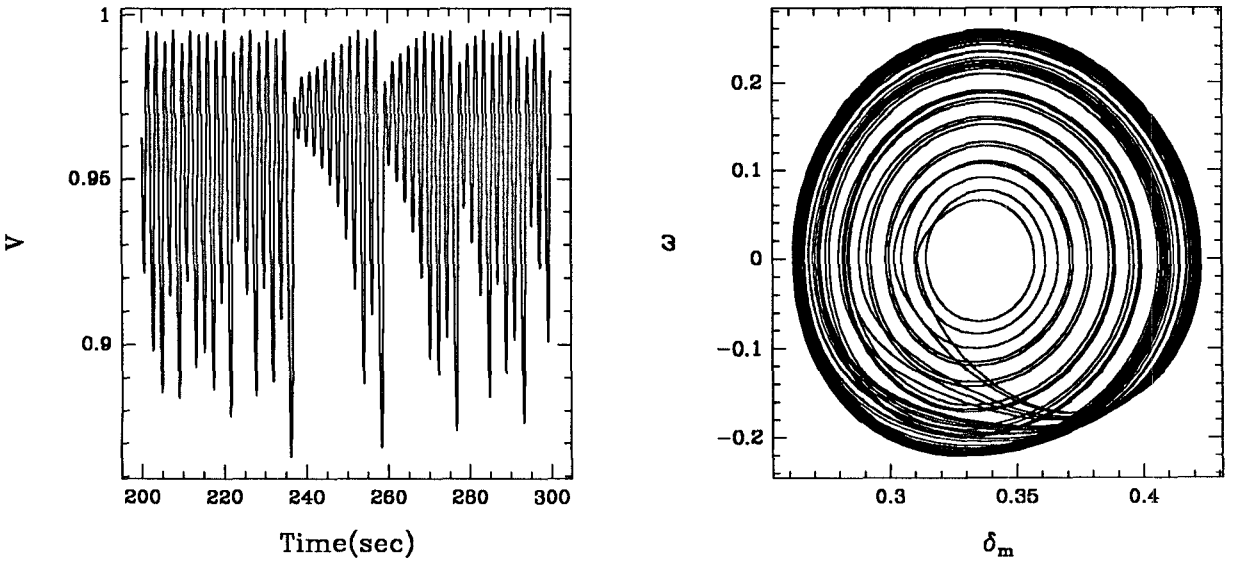

Figure 4: A chaotic orbit for $Q_1 = 11.377$.

periodic branches, of higher and higher period, paralleling the single exhibited branch from PDB③ to PDB④. These consist almost entirely of unstable orbits. The stable dynamical behavior is chaotic—there is some kind of strange attractor. This is what is observed. In particular, we have observed chaotic orbits in the general vicinity of the bifurcations occurring at the far right in Fig. 2 (PDB④, HB⑤ and SNB⑥). Chaos is observed in the fourth order model in the approximate range $Q_1 = 11.377 - 11.3825$, and for the third order model in the approximate range $Q_1 = 11.38875 - 11.395$. Fig. 4 shows such a chaotic orbit for the fourth order system for the parameter value $Q_1 = 11.377$. (The initial condition used to generate this orbit is $(\delta_m = 0.3503, \omega = 0.001, \delta = 0.13899, V = 0.915)$.) Fig. 4a represents the time simulation of V vs. time, and Fig. 4b gives the corresponding simulation projected in phase space onto ω vs. δ_m coordinates. Note that, in reference [5], Liapunov exponents and power spectra are calculated as evidence for the presence of chaotic invariant sets.

4 Voltage Collapse

The bifurcations uncovered in the foregoing analysis are important to the dynamics of voltage collapse for the model power system under consideration. Fig. 5 shows an example of a typical voltage collapse for the third and fourth order models within the Hopf window. The same parameter value is used for both Fig. 5a and Fig. 5b, namely $Q_1 = 11.25$. The initial conditions used to generate the simulations of Figs. 5a and 5b are also in agreement. (Specifically, we take $(\delta_m = 0.3503, \omega = 0.001, \delta = 0.13899, V = 0.915)$ for Fig. 5a, and $(\delta_m = 0.3503, \omega = 0.001, V = 0.915)$ for Fig. 5b.) Note the oscillatory nature of the solution, and the more pronounced drop in V for the fourth order model (Fig. 5a) than for the third order model (Fig. 5b). Fig. 6 shows a simulation of a "cooked" example in which collapse occurs in a nonoscillatory fashion just after the first Hopf bifurcation point for the fourth order model (i.e., for Q_1 slightly greater than $Q_1^{①}$). The parameter value used for this simulation is $Q_1 = 11.0$. What is cooked about this example is the choice of initial conditions. For the same parameter value, "most" other choices of initial conditions near the nominal stationary point give rise to oscillatory collapse, of the type illustrated in Fig. 5.

Fig. 7 shows a typical collapse simulation near to the saddle node bifurcation, for the fourth order model. This is a very sharp collapse as predicted in [2]. However, it should be noted that this behavior only occurs if the initial condition is near the nominal equilibrium for parameter values near $Q_1^{⑥}$. Such an initial condition is hardly likely, since the previous bifurcations discussed above will have resulted in an excursion away from the nominal equilibrium. For the third order model, the collapse is not as sharp, and the voltage undergoes a small oscillation about zero after the collapse. This is not shown here, and in reality the model does not capture dynamics for small values of the voltage, since it should not allow for negative voltage magnitudes. Such voltage excursions occur for both the fourth order and the third order models.

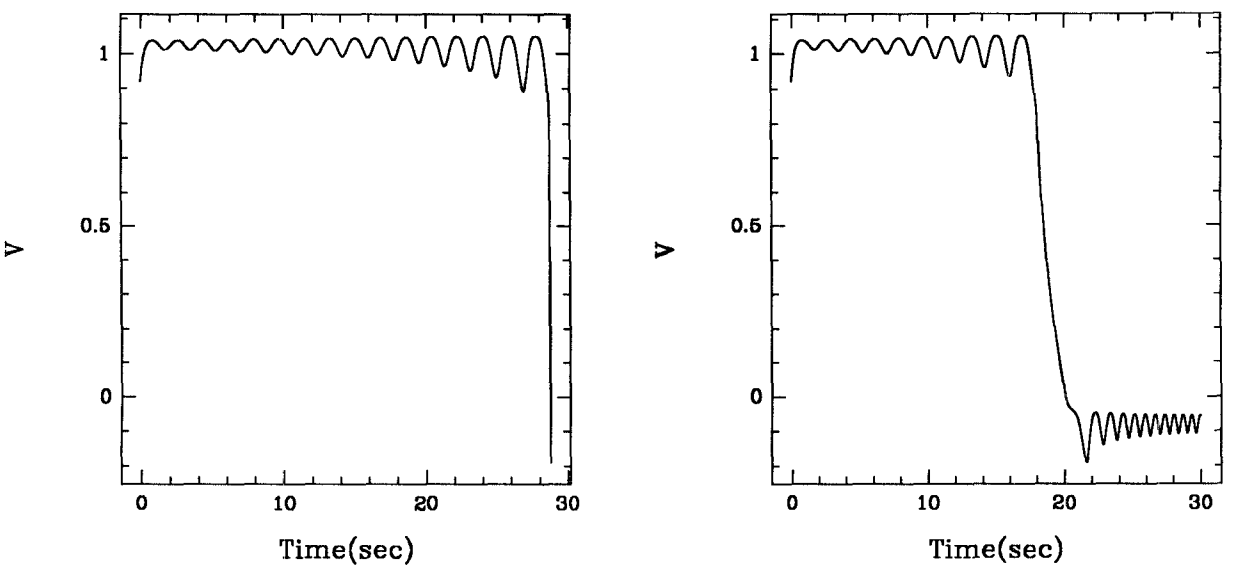

(a) Fourth order model (b) Third order model

Figure 5: Typical voltage collapse in Hopf window.

5 Conclusions

Bifurcations have been studied for a power system dynamic model which has previously been used to illustrate voltage collapse. It was found that for this model, the nominal operating point undergoes dynamic bifurcations prior to the static bifurcation to which voltage collapse has been attributed. These dynamic bifurcations result in a reduced stability margin in parameter space. Moreover, a short oscillatory voltage transient typically occurs prior to voltage collapse for this model. In addition, it was found that the model admits large amplitude bifurcations including cyclic fold and period doubling bifurcations; the latter leading to period doubling cascades and the resulting chaotic behavior. The relative importance of these effects in general power systems under stressed conditions is a topic for further research.

Acknowledgment

This research has been supported in part by the National Science Foundation's Engineering Research Centers Program: NSFD CDR-88-03012, by NSF Grant ECS-86-57561, by the TRW Foundation, and by the Power Engineering Program at the Dept. of Electrical Engineering, University of Maryland.

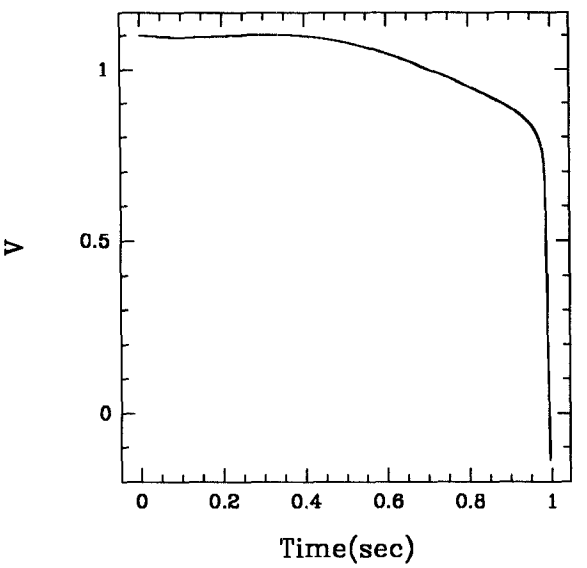

Fig. 6. "Cooked" voltage collapse in the Hopf Window.

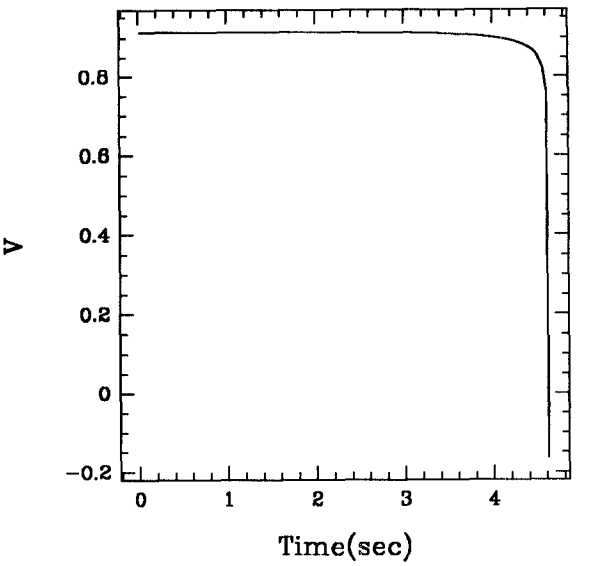

Fig. 7. Voltage collapse near the saddle node bifurcation.

References

[1] Y. Mansour, Ed., *Voltage Stability of Power Systems: Concepts, Analytical Tools, and Industry Experience*, New York: IEEE Press, (Publ. 90TH0358-2-PWR), 1990.

[2] I. Dobson and H.-D. Chiang, "Towards a theory of voltage collapse in electric power systems," *Systems and Control Letters*, Vol. 13, 1989, pp. 253-262.

[3] E.H. Abed, A.M.A. Hamdan, H.-C. Lee and A.G. Parlos, "On bifurcations in power system models and voltage collapse," *Proceedings of the 29th IEEE Conference on Decision and Control*, Honolulu, 1990, pp. 3014-3015.

[4] E.H. Abed, J.C. Alexander, H. Wang, A.M.A. Hamdan and H.-C. Lee, "Dynamic bifurcations in a power system model exhibiting voltage collapse," *Proceedings of the 1992 IEEE Int. Symp. on Circuits and Systems*, San Diego, 1992, to appear.

[5] H.-D. Chiang, C.-W. Liu, P.P. Varaiya, F.F. Wu and M.G. Lauby, "Chaos in a simple power system," Paper No. 92 WM 151-1 PWRS, *IEEE Winter Power Meeting*, 1992.

[6] K.T. Vu and C.C. Liu, "Dynamic mechanisms of voltage collapse," *Systems and Control Letters*, Vol. 15, 1990, pp. 329-338.

[7] J.C. Chow, R. Fischl and H. Yan, "On the evaluation of voltage collapse criteria," *IEEE Trans. on Power Systems*, Vol. 5, 1990, pp. 612-620.

[8] R.L. Devaney, *An Introduction to Chaotic Dynamical Systems*, Second Edition, Addison-Wesley, Redwood City, CA, 1989.

[9] J.E. Marsden and M. McCracken, *The Hopf Bifurcation and Its Applications*, New York: Springer-Verlag, 1976.

[10] B.D. Hassard, N.D. Kazarinoff and Y.-H. Wan, *Theory and Applications of Hopf Bifurcation*, Cambridge, U.K.: Cambridge University Press, 1981.

[11] J.M.T. Thompson and H.B. Stewart, *Nonlinear Dynamics and Chaos*, Chichester, U.K.:John Wiley and Sons, 1986.

[12] H.-D. Chiang, I. Dobson, R.J. Thomas, J.S. Thorp and L. Fekih-Ahmed, "On voltage collapse in electric power systems," *IEEE Trans. on Power Systems*, Vol. 5, 1990, pp. 601-611.

[13] F.M.A. Salam, J.E. Marsden and P.P. Varaiya, "Arnold diffusion in the swing equations of a power system," *IEEE Trans. Circuits and Systems*, Vol. CAS-31, 1984, pp. 673-688.

[14] M.A. Nayfeh, A.M.A. Hamdan and A.H. Nayfeh, "Chaos and instability in a power system: Primary resonant case," *Nonlinear Dynamics*, Vol. 1, pp. 313-339, 1990.

[15] E.J. Doedel, "AUTO: A program for the automatic bifurcation analysis of autonomous systems," *Cong. Num.*, Vol. 30, pp. 265-284, 1981.

[16] J. Guckenheimer and S. Kim, *kaos: Dynamical System Toolkit with Interactive Graphic Interface*, Mathematics Dept., Cornell Univ., Ithaca, NY, 1990.

[17] H.G. Kwatny, A.K. Pasrija and L.Y. Bahar, "Static bifurcation in electric power networks: Loss of steady-state stability and voltage collapse," *IEEE Trans. Circuits Syst.*, Vol. CAS-33, pp. 981-991, 1986.

[18] E.H. Abed and P.P. Varaiya, "Nonlinear oscillations in power systems," *Int. J. Elec. Power and Energy Syst.*, Vol. 6,. pp. 37-43, 1984.

[19] G. Rajagopalan, P.W. Sauer and M.A. Pai, "Analysis of voltage control systems exhibiting Hopf bifurcation," *Proc. 28th IEEE Conf. Dec. Contr.*, Tampa, pp. 332-335, 1989.

[20] V. Venkatasubramanian, H. Schättler and J. Zaborszky, "Voltage dynamics: Study of a generator with voltage control, transmission and matched MW load," *IEEE Trans. Automatic Control*, to appear.